

**ORIGINAL RESEARCH**

## Intravenous and Intratracheal Mesenchymal Stromal Cell Injection in a Mouse Model of Pulmonary Emphysema

Jeroen Tibboel,<sup>1,3</sup> Richard Keijzer,<sup>4</sup> Irwin Reiss,<sup>3</sup> Johan C. de Jongste,<sup>3</sup> and Martin Post<sup>1,2</sup>

1 Department of Physiology and Experimental Medicine, Hospital for Sick Children, Toronto, Canada

2 Department of Laboratory Medicine and Pathobiology, University of Toronto, Toronto, Canada

3 Department of Pediatrics, Erasmus University Medical Center – Sophia Children's Hospital, Rotterdam, The Netherlands

4 Department of Pediatric General Surgery, Manitoba Institute of Child Health, Winnipeg, Canada

### Abstract

The aim of this study was to characterize the evolution of lung function and -structure in elastase-induced emphysema in adult mice and the effect of mesenchymal stromal cell (MSC) administration on these parameters. Adult mice were treated with intratracheal (4.8 units/100 g bodyweight) elastase to induce emphysema. MSCs were administered intratracheally or intravenously, before or after elastase injection. Lung function measurements, histological and morphometric analysis of lung tissue were performed at 3 weeks, 5 and 10 months after elastase and at 19, 20 and 21 days following MSC administration. Elastase-treated mice showed increased dynamic compliance and total lung capacity, and reduced tissue-specific elastance and forced expiratory flows at 3 weeks after elastase, which persisted during 10 months follow-up. Histology showed heterogeneous alveolar destruction which also persisted during long-term follow-up. Jugular vein injection of MSCs before elastase inhibited deterioration of lung function but had no effects on histology. Intratracheal MSC treatment did not modify lung function or histology. In conclusion, elastase-treated mice displayed persistent characteristics of pulmonary emphysema. Jugular vein injection of MSCs prior to elastase reduced deterioration of lung function. Intratracheal MSC treatment had no effect on lung function or histology.

### Introduction

Chronic Obstructive Pulmonary Disease (COPD) is the most common chronic lung disease in adults, characterized by an incompletely reversible airflow limitation, and is associated with high mortality (1) and health-care costs (2). Pulmonary emphysema is an important component of COPD, and is characterized by alveolar destruction, resulting in a reduced alveolar surface area and increased alveolar size (3). Not all patients with pulmonary emphysema exhibit airflow limitation, respectively COPD (4), showing that there is a discrepancy between lung function and histological abnormalities. Oxidative stress, sustained inflammation and protease-antiprotease imbalance (5) are believed to be major contributors to the pathogenesis of COPD. To date no curative therapy is available, and smoking cessation and domiciliary oxygen supplementation only prolong survival in a small subset of patients with resting PaO<sub>2</sub> < 60 mmHg (6).

Mesenchymal stromal cells have recently emerged as a successful, cell-based therapy in a variety of models of lung disease, such as hyperoxia (7), bleomycin (8) and endotoxin-induced lung injury (9). MSCs are

**Keywords:** MSC, elastase, histology, morphometry, jugular vein

**Correspondence to:** Martin Post, Ph.D., The Hospital for Sick Children, 555 University Avenue, Toronto, ON M5G 1X8, phone: (416) 813-6772, fax: (416) 813-5002, email: martin.post@sickkids.ca

multipotent stromal cells that have the ability to self-renew. The hypothesis for the mechanism underlying the beneficial effects of MSC treatment has shifted from engraftment and differentiation of MSCs in the target organ towards the effects of paracrine factors produced by these MSCs (10). Levels of engraftment below 1% were found in several studies (11–14).

Thus, it is highly unlikely that engraftment is responsible for the favourable effects of MSCs in various models of lung injury (11,15–17). MSC have been shown to inhibit apoptosis (18) and secrete anti-inflammatory mediators (19) and growth factors, such as epidermal growth factor (20) and hepatocyte growth factor (21). It has been shown that the intravenous infusion of conditioned medium, derived from MSCs, prevents LPS-induced lung injury, supporting that MSCs exert their effect via paracrine signalling (22).

Katsha et al. have shown that treatment with MSCs improves histological and morphometrical outcome in a low dose elastase-induced emphysema model (1 Unit/100 gram bodyweight) and decreases inflammatory cytokine levels (23). Also Cruz et al. have shown that injection of bone marrow mononuclear cells (BMNCs) improves histological and morphometrical outcome in a low dose (4 times 0.4 Units/100 gram bodyweight) elastase model (24). Based on the results of MSC treatment in different animal models, a phase II-trial of intravenous mesenchymal stem cell infusion in COPD patients was started in 2008. The interim report of this study stated that, although this treatment was safe and reduced C-reactive protein levels, lung function in these patients did not improve (25).

The absence of an improvement in lung function suggests that MSCs did not repair the structural defect (26). Since these human trial findings were not in line with the aforementioned animal studies (23,24), the question arises whether the animal models may not mimic human COPD, and that a better response to MSC is seen because of a lower level of lung damage. One possibility is that the elastase dose had been too low to cause the desired level of alveolar damage. We, therefore, examined the effects of MSC treatment in a mouse model of emphysema, using a relatively high dose of elastase (4.8 Units / 100 gram bodyweight). Because some previous studies (24,25) used an intravenous route of MSC administration, yet others (23) used intratracheal delivery, we tested both methods of administration of MSCs, aiming at either prevention or repair of lung injury.

## Methods

### Animals

All animals were obtained from Charles River (St. Constant, Quebec, Canada). Animal studies were conducted according to the criteria established by the Canadian Council for Animal Care and approved by the

Animal Care and Use Committee of the Hospital for Sick Children, Toronto, ON, Canada. Adult C57/BL6 mice were used for all experiments described below, except for the extraction of MSCs from bone marrow, for which 4-week-old C57/BL6 mice were used.

### Elastase-induced lung injury

Porcine pancreatic elastase (Type I, aqueous suspension,  $\geq 4.0$  units/mg protein, Calbiochem, EMD biosciences USA) was dissolved in sterile saline to create a total volume for injection of 100  $\mu$ L per mouse, with a concentration of 4.8 Units/100 g bodyweight, a dosage used previously (27–29). Animals were anesthetized with 3% isoflurane and *ip* administration of 75 mg/kg ketamine (75 mg/kg) and 5 mg/kg xylazine (5 mg/kg). Following induction of anesthesia, a 25 G intubation tube was inserted past the vocal cords, and 100  $\mu$ L of elastase was injected into the trachea. Control animals were treated similarly, but received sterile saline instead of elastase.

### Mesenchymal stromal cell extraction and characterization

Bone marrow was collected from 4-week-old C57/BL6 mice. Mice were sacrificed by cervical dislocation, and the tibia and femur removed, from which the bone marrow was extracted by flushing through Dulbecco's Modified Eagle Medium (DMEM). The suspension was filtered using a 70- $\mu$ m sterile filter before being cultured using StemXVivo Mesenchymal Stem Cell expansion medium (R&D systems, Minneapolis, USA) according to a modified protocol (30). Mesenchymal stromal cells were isolated by plastic adherence, and prior to injection, passage 8 adherent MSCs were characterized using flow cytometry.

MSCs characterized according to the International Society of Cellular Therapy consensus in 2006 must fulfill the following three criteria: (1) MSC must be adherent to plastic under standard tissue culture conditions; (2) MSC must express the cellular markers CD73, CD90 and CD105, and must not express CD34, CD45, CD14 or CD11b; and (3) MSC must have the capacity to differentiate into mesenchymal lineages under *in vitro* conditions (31). Adherent cells were collected from their culture flasks by trypsin digestion and a subset of cells were stained with primary conjugated antibodies for CD34, CD45, CD73, CD105 and Sca-1 (Miltenyi Biotec, Bergisch Gladbach, Germany) according to manufacturer's protocol. Expression of the above mentioned markers was characterized using a Gallios flow cytometer (Beckman Coulter, Mississauga, Canada).

A differentiation assay was performed on passage 8 MSCs to test their multi-lineage differentiation capacity. According to a protocol by Lama et al. (32), MSCs were cultured in different media to obtain adipogenic, chondrogenic, and osteogenic differentiation. Adipogenic: DMEM + 1  $\mu$ M dexamethasone + 10  $\mu$ M insulin + 200  $\mu$ M indomethacin + 0.5 mM isobutyl-methyl xanthine. Chondrogenic: DMEM + 10 ng/mL TFG- $\beta$ 1. Osteogenic:

DMEM + 100 nM dexamethasone + 10 mM beta-glycerophosphate + 0.05 mM ascorbic acid-2-phosphate. Histological staining for adipocytes (Oil-red stain), osteoblasts (Von Kossa stain) and chondrocytes (Alcian Blue stain) were performed according to a previously published protocol (32).

### Mesenchymal stromal cell administration

MSCs were dissolved in plasmalyte (Baxter, Mississauga, Canada) at a concentration of 500,000 cells per 200  $\mu$ L for intratracheal instillation and at a concentration of 100,000 cells per 100  $\mu$ L jugular vein injection.

### Intratracheal instillation of MSCs

Animals were anesthetized with 3% isoflurane and *ip* administration of 75 mg/kg ketamine (75 mg/kg) and 5 mg/kg xylazine (5 mg/kg). Following induction of anesthesia, a 25 G intubation tube was inserted past the vocal cords and 500,000 MSCs suspended in 200  $\mu$ L of plasmalyte were injected into the trachea. Control animals were treated similarly, but received plasmalyte only. To test whether MSCs could prevent elastase-induced lung injury, intratracheal MSC installation was performed 24 hours before elastase injection in experimental group 1, and 24 hours after elastase injection in experimental group 2. To test whether MSC's could repair elastase-induced lung injury, intratracheal MSC installation was also performed 21 days after elastase treatment (Figure E1 of the online supplement).

### Infusion of MSCs via the jugular vein

Animals were anesthetized with 3% isoflurane, which was maintained during the entire procedure. The jugular vein was exposed and 100,000 MSCs suspended in 100  $\mu$ L plasmalyte were slowly infused. Pressure was applied on the jugular vein until bleeding ceased, the wound was sutured and the animals were allowed to recover. Jugular vein MSC infusion was performed 30 minutes before intratracheal elastase injection.

### Lung function measurements

At multiple time points (Figure E1 of the online supplement) following the instillation of elastase and/or MSC treatment, unrestrained whole body plethysmography (Buxco Research Systems, Wilmington, NC, USA) was used to measure breathing frequency, tidal volume and minute volume. Afterwards the Flexivent rodent ventilator (Scireq, Montreal, Canada) was used to invasively assess lung function (described in detail in the online supplement) following a protocol previously published (33).

### Bronchoalveolar lavage

A subset of mice was used to obtain BAL samples only. Immediately after sacrificing the animal, the lungs were lavaged at 6 hours, and 1–5, 8, 14 and 21 days after elastase injection through a separate endotracheal tube

with 3  $\times$  600  $\mu$ L sterile saline, followed by withdrawal (34,35). The collected pooled aliquots were centrifuged at 1400 *g* for 8 minutes. The supernatant was collected for cytokine analysis.

### Measuring cytokines

Cytokines were measured in BAL fluid using xMAP technology on a Luminex 200 (Luminex Corporation, Austin, Texas, USA) using a milliplex kit from EMD Millipore Corporation (Billerica, Massachusetts, USA) according to the manufacturers protocol. The following analytes were measured: IL-1 $\beta$ , IL-6, IL-10, IL-13, MCP-1, TNF- $\alpha$ , KC, GM-CSF.

### Histology of the lungs

Following lung function measurements histology was performed as described in the online supplement.

### Statistics

All values are presented as mean  $\pm$  standard error of the mean when normally distributed (Sigmaplot version 11 for Windows). Differences were assessed by Student's *t*-test or, for comparison of more than two groups, by one-way analysis of variance, followed by Tukey HSD comparison test. *p*-values below 0.05 were considered significant.

## Results

### Elastase-induced alveolar injury

Elastase-treated mice showed significant decreases in resistance and tissue-specific elastance, and significant increases in dynamic compliance, total lung capacity and static compliance when compared to saline-treated mice. Forced expiration measurements revealed a significant increase in forced vital capacity and a significant decrease in mean forced expiratory flow in elastase-treated mice (Figure 1, Table E1 of the online supplement). At 5 months and 10 months after elastase instillation, the increase in dynamic compliance and FVC, as well as the decrease in tissue-specific elastance and forced expiratory flows seen at 3 weeks after elastase had persisted (Figure 2, Table E2 of the online supplement).

No significant changes in plethysmographic lung function parameters were found when compared to saline-treated controls (Table E2 of the online supplement). Histology at 21 days after elastase showed a heterogeneous pattern of alveolar destruction with enlarged airspaces. This was reflected in a significant increase in mean linear intercept and a reduced alveolar number. No significant change in radial alveolar count was detected. Histological analysis of lungs at 5 and 10 months after elastase treatment revealed a persistent, heterogeneous pattern of enlarged airspaces and an increased mean linear intercept (Figure 3).

Elastin staining at 21 days after elastase administration showed a disorganized pattern of elastin distribution in

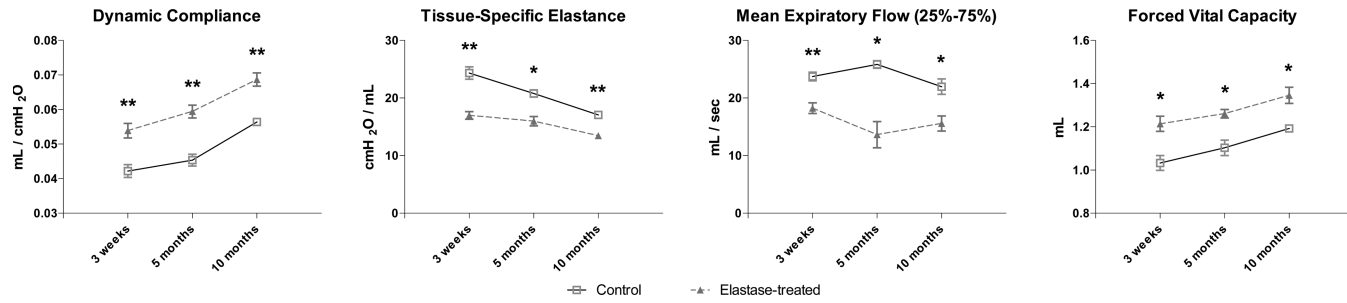


Figure 1. Lung function measurements 21 days after elastase instillation (n = 30) and in saline controls (n = 25). Data are expressed as mean ± SEM. \* = p < 0.05.

elastase-treated mice compared to controls. No significant difference in elastin content per total tissue area was observed (Figure 4). Histological slides of elastase-treated mice showed influx of inflammatory cells, and cytokine levels in BAL fluid showed a transient increase in IL-6, keratinocyte-derived-chemokine (KC) and MCP-1 levels at day 2 after elastase injection. Cytokine levels returned to baseline at day 3 and remained stable for the follow up period of 3 weeks. Levels of IL-1β,

IL-10, IL-13 and GM-CSF were below the detectable range (Figure 5, Table E3 of the online supplement).

**Mesenchymal stromal cell characterization**

Passage 8-adherent bone marrow stromal cells were characterized by differentiation assay and showed differentiation into adipocytes, chondrocytes and cartilage. Flow cytometry revealed that a subset of bone marrow cells was positive for CD105 (28.2%), CD73 (28.8%), CD90 (69.2%) and

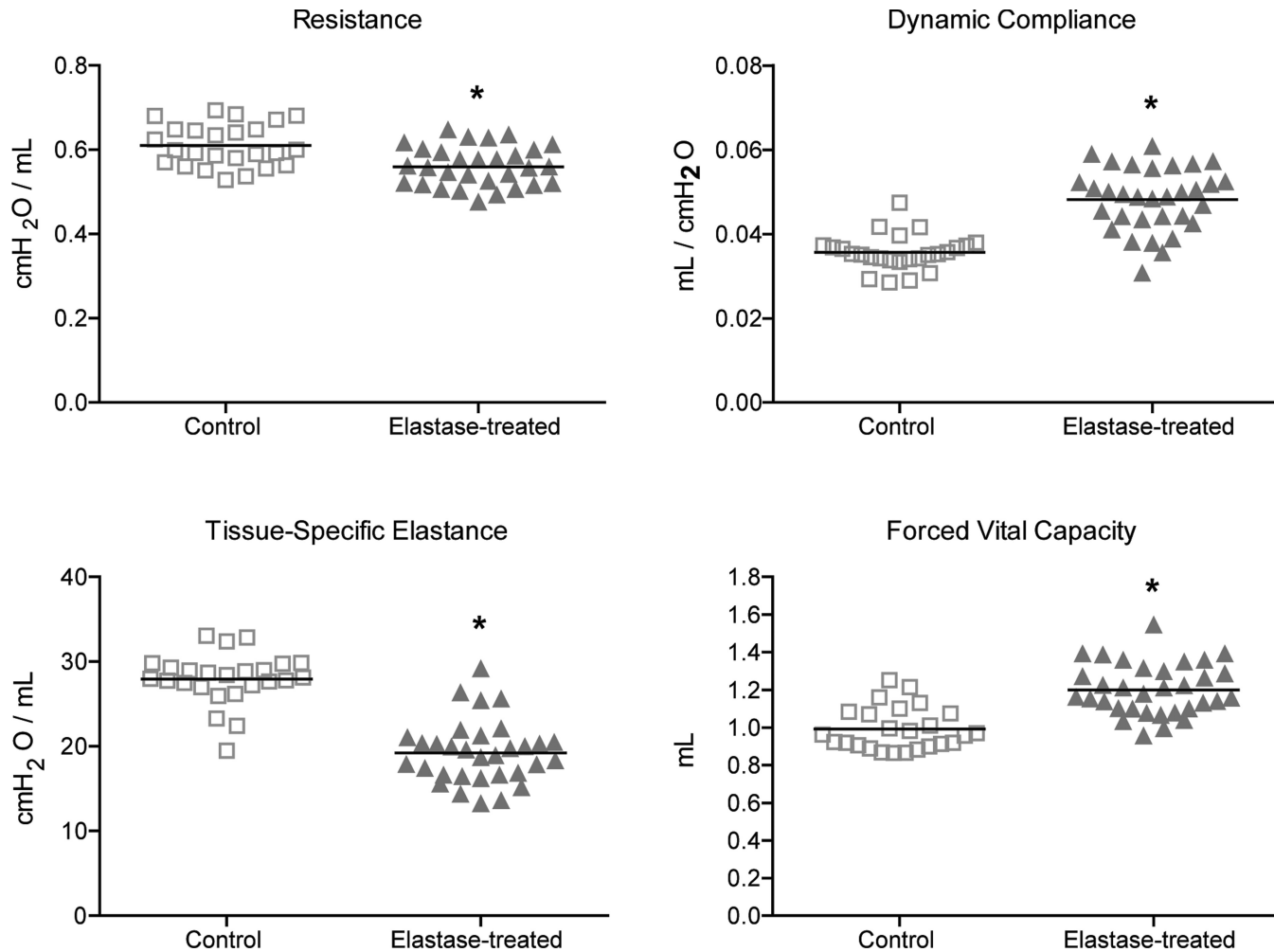
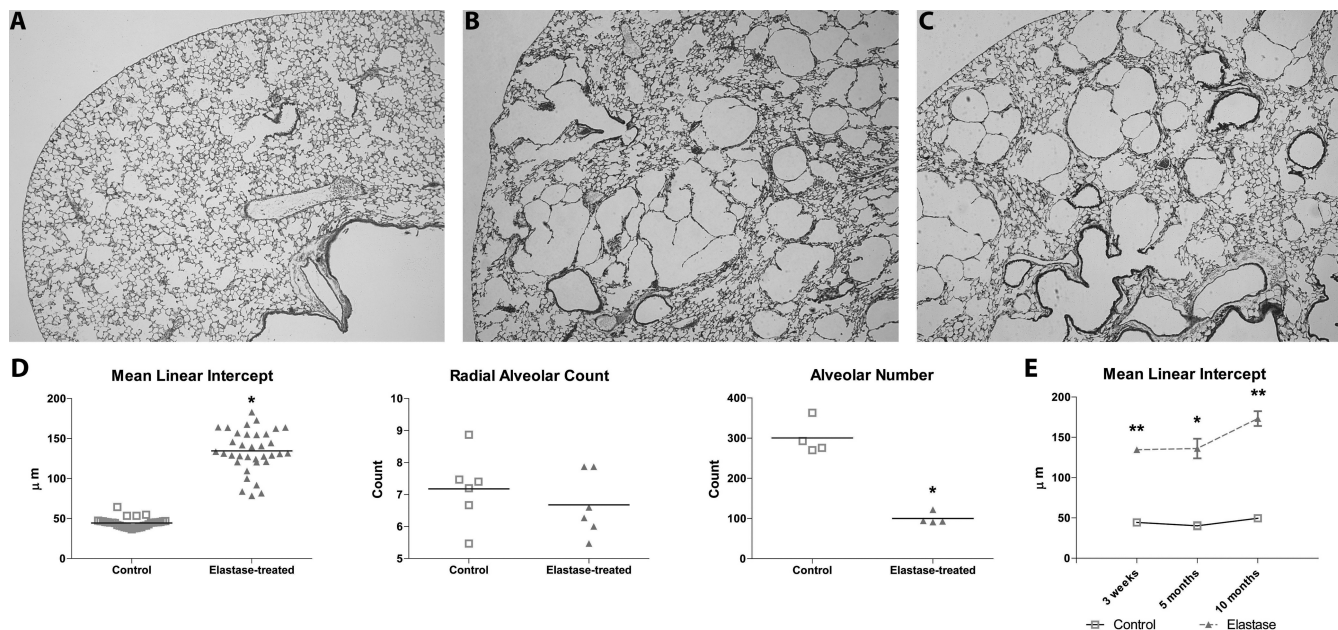


Figure 2. Lung function measurements during long-term follow-up of elastase-treated mice (n = 30 for 21 days, n = 5 for 5 and 10 months) and saline controls (n = 25 for 21 days, n = 5 for 5 and 10 months). Data are expressed as mean ± SEM. \* = p < 0.05. \*\* = p < 0.01.



**Figure 3.** Representative histological sections of saline-controls (A), elastase-treated mice 21 days after injection (B) and elastase-treated mice 10 months after elastase injection (C). Sections were stained with hematoxylin and eosin. Morphometry results (D) are expressed as mean  $\pm$  SEM for both control and elastase-treated group for mean linear intercept (n = 35), radial alveolar counts (n = 6), and alveolar number (n = 4). Morphometry results for 5 and 10 months of recovery in room-air (E) are expressed as mean  $\pm$  SEM for mean linear intercept (n = 5). \* =  $p < 0.05$  \*\* =  $p < 0.001$ .

Sca-1 (99.5%) and negative for CD34 (0%) and CD45 (0%) (Figure E2 of the online supplement).

#### Intratracheal MSC instillation

Intratracheal instillation of  $5 \times 10^5$  of MSCs at 24 hours before, and at 24 hours or 21 days after elastase treatment had no effect on lung function or histology performed 21 days after MSC injection (Figure E3, Table E4 of the online supplement).

#### Intravenous MSC infusion

Infusion of  $10^5$  MSCs 30 minutes before intratracheal instillation of elastase ameliorated the increase in dynamic compliance and tissue-specific elastance in elastase-treated animals compared to controls (Figure 6, Table E4 of the online supplement). Intravenous MSC

infusion had no effect on histology or morphometry (Figure E3 of the online supplement).

## Discussion

In this study, we induced pulmonary emphysema in adult mice by tracheal instillation of a relatively high dose of elastase. Three weeks after elastase administration we found evidence of histological abnormalities and obstructive lung function, characteristic of pulmonary emphysema. The structural and functional changes persisted up to 10 months and were not affected by intratracheal administration of MSC prior or after the injury. Jugular vein MSC treatment before elastase injection showed an improvement in lung function but no change in histology.

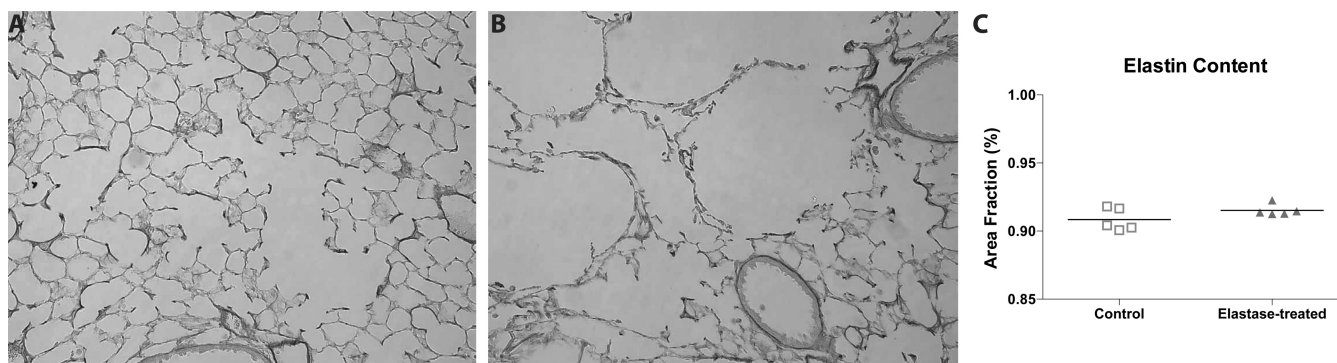


**Figure 4.** Hart's Elastin stain of histological slides of the lungs of saline-treated (A) and elastase-treated mice (B) 21 days after injection. Morphometry shows the quantification of the elastin content when adjusted for total tissue area (C). All morphometrical data is expressed as mean  $\pm$  SEM, n = 5 for control and elastase-treated mice. # =  $p < 0.05$ .

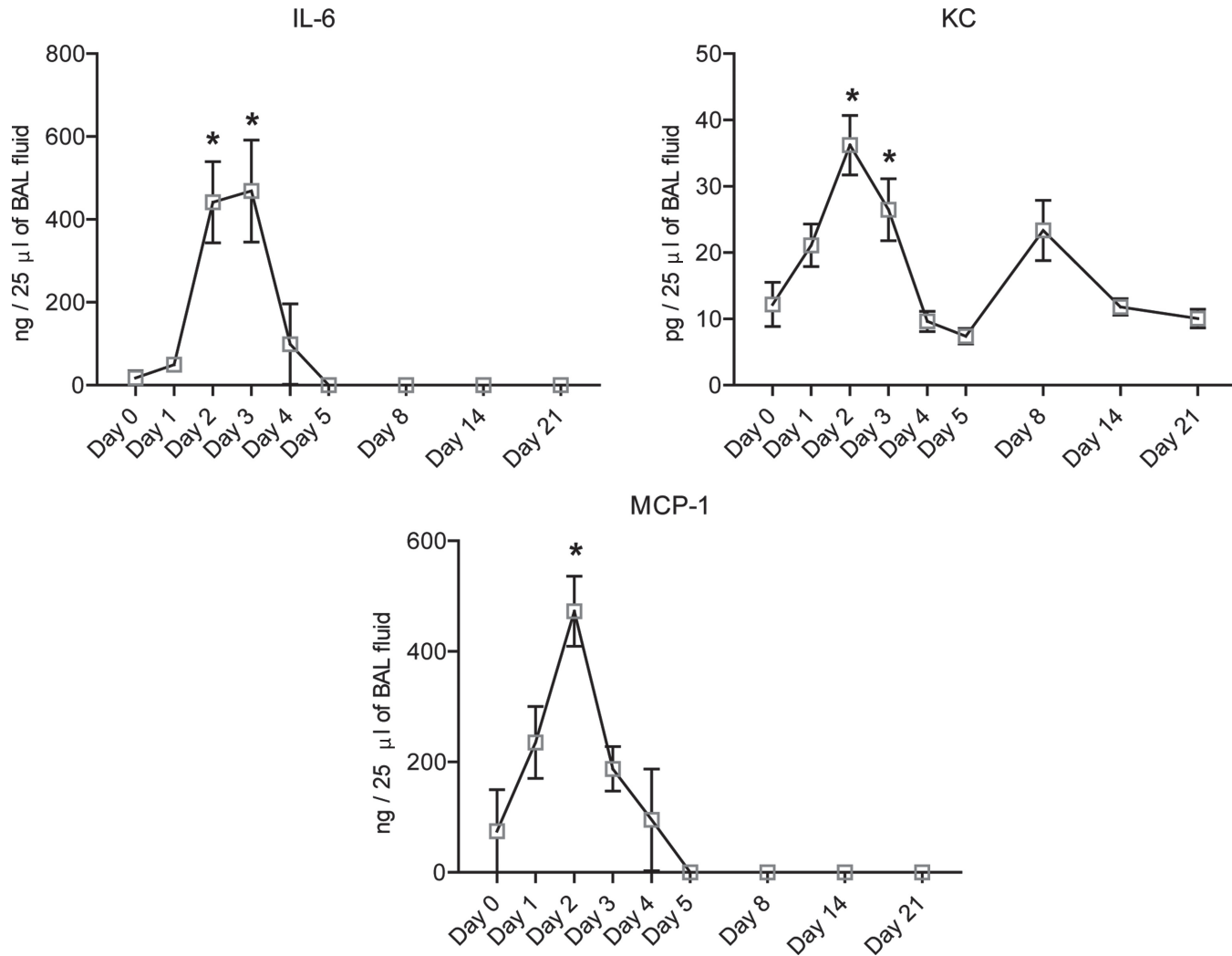


**Figure 5.** Measurement of cytokine levels in BAL fluid after elastase injection show a significant increase in MCP-1 levels at day 2 after elastase injection and a significant increase in IL-6 and KC levels at day 2 and 3 after elastase injection. Results represent a total of 4 mice per group for all time-points. \* =  $p < 0.05$ .

Intratracheal instillation of elastase resulted in increased dynamic compliance, total lung capacity, FVC and decreased tissue-specific elastance and forced expiratory flows 3 weeks after elastase injection. These results

agree with earlier findings at 3 weeks after elastase injection (36–38) and are likely due to a loss of elastin and disruption of the integrity of the alveolar wall with loss of alveolar attachments. Indeed, we observed extensive

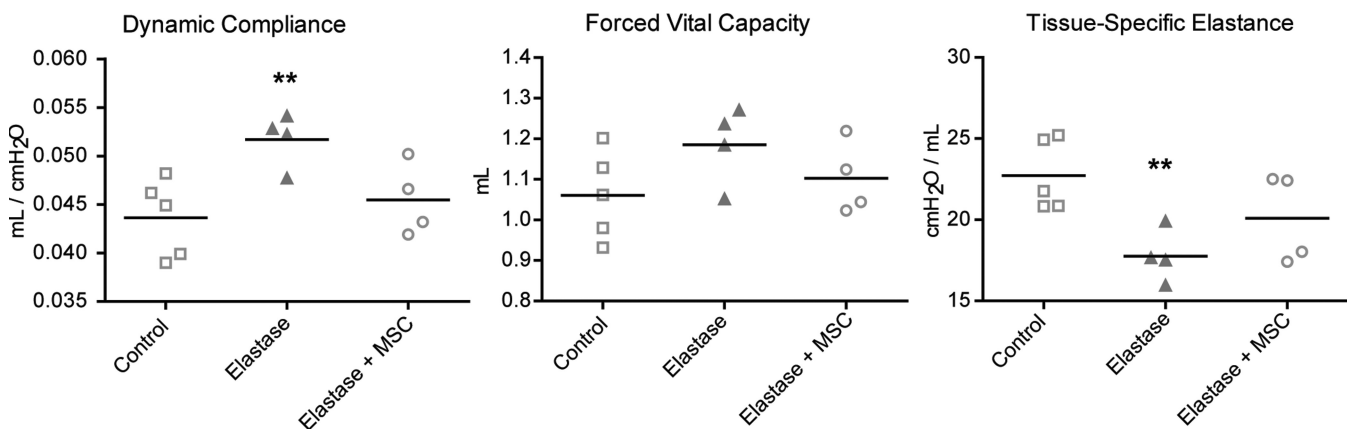


**Figure 6.** Lung function measurements 21 days after elastase instillation (n = 5), elastase instillation + jugular vein MSC injection (n = 4) and in saline controls (n = 4). Data are expressed as mean  $\pm$  SEM. \*\* =  $p < 0.05$ .

alveolar damage. Hart's staining on lung tissue showed a disorganized elastin deposition after elastase treatment. Disorganisation of elastin fibers and loss of alveolar attachments reduces elastic recoil of the lung. This is likely to contribute to the decreases in forced expiratory flows, as well as to the static hyperinflation.

Loss of structural integrity of the peripheral lung with disruption of the alveolar walls and loss of alveolar attachments could also be responsible for the increase in total lung capacity (TLC). A possible mechanism of increased TLC could be air trapping. However, we consider this unlikely, because the simultaneous increase in FVC argues against substantial air trapping. Note that the forced lung function manoeuvres performed in this study differ from those used in clinical setting because we used a negative pressure at the tracheal opening, whereas in human subjects the driving force is a positive pressure from the diaphragm and thoracic wall. This negative pressure could lead to earlier airway collapse and more pronounced airway obstruction than active forced exhalation.

In the present study, we used both non-invasive and invasive lung function measurements. Non-invasive measurements are advantageous in longitudinal studies in which animals can be repeatedly measured, but the overall sensitivity for detecting lung function abnormalities appeared lower than that of invasive measurements (39). The invasive measurements were more robust and sensitive, and accurately reflected alterations in lung mechanics. Thus, the Flexivent method was superior for detecting physiological differences in lung mechanics in mice with elastase-induced lung injury, in agreement with earlier findings in hyperoxia-induced lung injury (40). The main advantage of whole body plethysmography is its repeatability. However, de Vleeschauwer *et al.* have recently shown that intubating mice for repeated invasive measurements yielded the same results as performing a tracheotomy (41) and therefore for we consider Flexivent measurements the method of choice for future experiments.

To our knowledge, no long-term functional measurements have been performed in the elastase-induced mouse model of emphysema. During long term follow-up, we found no evidence of recovery of lung injury. This suggests that the elastase model is suitable for intervention studies aimed at tissue repair. The repeated use of lung function measurements in this model enables us to monitor disease progression and treatment efficacy in a manner that may be relevant to clinical practice.

The findings with the forced expiration measurements do not agree with all other findings reflecting emphysema. We think that this might well be due to the smaller number of animals used for the forced expiratory measurements, and the relatively large variation within the groups. Overall, these measurements suggest that forced expiration measurements are less sensitive, with a larger variation between animals in the same group, than the other lung function measurements obtained with the Flexivent system.

In our emphysema model, intratracheal MSC installation shortly after elastase injection, aiming to prevent lung injury, had no effect on lung function or histology. We chose the intratracheal route to ensure that the injected MSCs came into direct contact with the damaged alveolar epithelial layer. This intratracheal approach was successfully applied in the study by Katsha *et al.* (23). As mentioned before, our elastase dose was significantly greater than that of Katsha *et al.*, which might account for the difference in outcome of MSC treatment. We have repeated the intratracheal MSC experiments in a rat model of emphysema (elastase dose: 30 Units / 100 g bodyweight) and  $5 \times 10^5$  rat bone marrow-derived MSCs (data not shown). These experiments also showed no effect of intratracheal MSC treatment on lung function, histology and morphometry, indicating that our results are reproducible in different species.

We also administered MSCs intratracheally 21 days after elastase injection to induce repair of elastase-induced lung injury. MSC injection had no effect on lung function or histology. The discrepancy between our negative results of repair by MSCs and those of others, with long-lasting low grade inflammation in a low-dose elastase model and effects of intratracheal MSC injection shortly after elastase (7,8,20,42), may be due to the absence of a persisting inflammatory component in our emphysema model. Since MSCs have been shown to possess anti-inflammatory properties, administering them 21 days after elastase injection, when cytokine levels had normalized, might reduce their ability to exert positive effects on lung function and histology.

COPD has been shown to possess a large vascular disease component (48). CT images of COPD patients show a decrease in small pulmonary vessels, even in smokers with mild emphysema (49). Compared to non-smokers, COPD patients show increased invasion of inflammatory cells in the vascular adventitial layer (50). The extent of pulmonary vascular remodelling directly correlates with the severity of the endothelial inflammation (51). Intravenous injection of MSCs creates a systemic anti-inflammatory response via the systemic circulation on the endothelial surface of the pulmonary vasculature. Thus, the anti-inflammatory milieu on the endothelial side produced by MSCs injected via the jugular vein could decrease the vascular inflammation shown to be present in the elastase-induced emphysema model (52). There is a large body of work suggesting that MSC intervention using the endothelial route, either via the dorsal penile vein (43) or via the tail vein (8,19,44) could be successful in improving elastase-induced emphysema, thereby improving lung function. We used the jugular vein infusion method to infuse the cells closest to the pulmonary vasculature. Jugular vein infusion of  $10^5$  MSCs just prior to elastase installation to prevent elastase-induced lung injury significantly improved lung function in elastase-treated mice, while histology did not improve. Another possible explanation is that MSCs

may have improved surfactant production or activity. It is well known that alveolar inflammation decreases surfactant production and activity (45–47) and as MSCs have an anti-inflammatory effect they may have improved surfactant production or activity and thereby improved lung function in the absence of histological improvement.

This hypothesis is less likely, since intratracheal injection of MSCs showed no improvement in lung function. Delivery of MSCs directly into the alveolar spaces should generate a local anti-inflammatory effect, thereby improving surfactant function. This effect was not seen in the intratracheal injection groups. More work is needed to study the underlying mechanism responsible for the improvement in lung function after jugular vein injection of MSCs.

In contrast to our work, Cruz *et al.* showed that intravenous injection of bone marrow mononuclear cells 3 hours after elastase injection decreased inflammatory parameters, but also improved histology and morphometry (24). Unfortunately, they did not measure lung function. The main difference in methodology between our study and the study of Cruz *et al.* is that they used a much lower dose of elastase, resulting in less alveolar enlargement, as measured by a MLI score of 68.5 compared to our MLI score of 128. The difference in alveolar destruction severity might account for the difference in treatment outcome, with our higher elastase dose surpassing the injury threshold for an effect of MSC treatment on histology and morphometry.

A major limitation of our study is the difference in timing of intravenous and intratracheal MSC injection, which invalidates comparison of the two interventions in the present study. Future studies are needed to examine whether the intravenous route might be beneficial after elastase. Another limitation is the different cell numbers used for intratracheal MSC injections when compared to jugular vein MSC injections. Unfortunately, we were limited in the number of cells for jugular vein injection because of 100% injection-induced mortality when using higher doses, as used for intratracheal MSC injections.

## Conclusion

Our results demonstrate that MSC injection via the jugular vein just before elastase prevented lung function changes after elastase treatment. Intratracheal administration 24 hours before and 24 hours after elastase injection did not prevent lung function changes. The severity of elastase-induced lung injury may be an important determinant of the effect of MSC treatment.

## Declaration of Interest Statement

The authors report no conflicts of interest. The authors alone are responsible for the content and writing of the paper.

## References

1. Mannino DM, Braman S. The epidemiology and economics of chronic obstructive pulmonary disease. *Proc Amer Thorac Soc* 2007; 4(7):502–506.
2. Faulkner MA, Hilleman DE. The economic impact of chronic obstructive pulmonary disease. *Exp Opin Pharmacother* 2002; 3(3):219–228.
3. Baraldo S, Turato G, Saetta M. Pathophysiology of the small airways in chronic obstructive pulmonary disease. *Respir Inter Rev Thorac Dis* 2012; 84(2):89–97.
4. Galbán CJ, Han MK, Boes JL, Chughtai KA, Meyer CR, Johnson TD, et al. Computed tomography-based biomarker provides unique signature for diagnosis of COPD phenotypes and disease progression. *Nature Med* 2012; 18(11):1711–1715.
5. Bourbon JR, Boucherat O, Boczkowski J, Crestani B, Delacourt C. Bronchopulmonary dysplasia and emphysema: in search of common therapeutic targets. *Trends Mol Med* 2009; 15(4):169–179.
6. Sin DDD, McAlister FFA, Man SFP, Anthonisen NR. Contemporary management of chronic obstructive pulmonary disease: Scientific review. *JAMA: J Amer Med Asso* 2003; 290(17):2301–2312.
7. Haafte T van, Byrne R, Bonnet S. Airway delivery of mesenchymal stem cells prevents arrested alveolar growth in neonatal lung injury in rats. *Amer J Respir Crit Care Med* 2009; 180:1131–1142.
8. Zhao F, Zhang Y, Liu Y, Zhou J, Li Z, Wu C, et al. Therapeutic effects of bone marrow-derived mesenchymal stem cells engraftment on bleomycin-induced lung injury in rats. *Transplant Proc* 2008; 40:1700–1705.
9. Gupta N, Su X, Popov B. Intrapulmonary delivery of bone marrow-derived mesenchymal stem cells improves survival and attenuates endotoxin-induced acute lung injury in mice. *J Immunol* 2007; 179(3):1855–1863.
10. Loebinger MR, Janes SM. Stem cells for lung disease. *Chest* 2007; 132(1):279–285.
11. Ortiz L a, Gambelli F, McBride C, Gaupp D, Baddoo M, Kaminski N, et al. Mesenchymal stem cell engraftment in lung is enhanced in response to bleomycin exposure and ameliorates its fibrotic effects. *Proc Natl Acad Sci USA* 2003; 100(14):8407–8411.
12. Rojas M, Xu J, Woods CR, Mora AL, Spears W, Roman J, et al. Bone marrow-derived mesenchymal stem cells in repair of the injured lung. *Amer J Respir Cell Mol Biol* 2005; 33(2):145–152.
13. Kotton DN, Fabian AJ, Mulligan RC. Failure of bone marrow to reconstitute lung epithelium. *Amer J Respir Cell Mol Biol* 2005; 33(4):328–334.
14. Loi R, Beckett T, Goncz KK, Suratt BT, Weiss DJ. Limited restoration of cystic fibrosis lung epithelium in vivo with adult bone marrow-derived cells. *Amer J Respir Crit Care Med* 2006; 173(2):171–179.
15. Yamada M, Kubo H, Kobayashi S, Ishizawa K, Numasaki M, Ueda S, et al. Bone marrow-derived progenitor cells are important for lung repair after lipopolysaccharide-induced lung injury. *J Immunol* 2004; 172(2):1266–1272.
16. Wong AP, Dutly AE, Sacher A, Lee H, Hwang DM, Liu M, et al. Targeted cell replacement with bone marrow cells for airway epithelial regeneration. *American journal of physiology. Lung Cell Mol Physiol* 2007; 293(3):L740–752.
17. Spees JL, Pociask D a, Sullivan DE, Whitney MJ, Lasky J a, Prockop DJ, et al. Engraftment of bone marrow progenitor cells in a rat model of asbestos-induced pulmonary fibrosis. *American journal of respiratory and critical care medicine*. 2007 Aug 15;176(4):385–94.
18. Block G, Ohkouchi S, Fung F, Frenkel J, Gregory C, Pochampally R, et al. Multipotent stromal cells are activated to reduce apoptosis in part of upregulation and



- secretion of stanniocalcin-1. *Stem Cells* 2009; 27(3):670–681.
19. Lee RH, Pulin A a, Seo MJ, Kota DJ, Ylostalo J, Larson BL, et al. Intravenous hMSCs improve myocardial infarction in mice because cells embolized in lung are activated to secrete the anti-inflammatory protein TSG-6. *Cell Stem Cell* 2009; 5(1):54–63.
  20. Chen L, Tredget EE, Wu PYG, Wu Y. Paracrine factors of mesenchymal stem cells recruit macrophages and endothelial lineage cells and enhance wound healing. *PLoS One* 2008; 3(4):e1886.
  21. Crisostomo PR, Wang Y, Markel T a, Wang M, Lahm T, Meldrum DR. Human mesenchymal stem cells stimulated by TNF-alpha, LPS, or hypoxia produce growth factors by an NF kappa B- but not JNK-dependent mechanism. *Amer J Physiol Cell Physiol* 2008; 294(3):C675–682.
  22. Ionescu L, Byrne RN, van Haften T, Vadivel A, Alphonse RS, Rey-Parra GJ, et al. Stem cell conditioned medium improves acute lung injury in mice: in vivo evidence for stem cell paracrine action. *Amer J Physiol Lung Cell Mol Physiol* 2012 Sep 28; 303:967–977.
  23. Katsha AM, Ohkouchi S, Xin H, Kanehira M, Sun R, Nukiwa T, et al. Paracrine factors of multipotent stromal cells ameliorate lung injury in an elastase-induced emphysema model. *Mol Ther J Amer Soc Gene Ther* 2011; 19(1):196–203.
  24. Cruz FF, Antunes MA, Abreu SC, Fujisaki LC, Silva JD, Xisto DG, et al. Protective effects of bone marrow mononuclear cell therapy on lung and heart in an elastase-induced emphysema model. *Respir Physiol Neurobiol* 2012; 182(1):26–36.
  25. Osiris. Osiris Therapeutics Reports interim data for COPD stem cell study. Available from: <http://investor.osiris.com/> 2012 Sep 05.
  26. Bouloukaki I, Tsiligianni IG, Tsoumakidou M, Mitrouska I, Prokopakis EP, Mavroudi I, et al. Sputum and nasal lavage lung-specific biomarkers before and after smoking cessation. *BMC Pulmon Med* 2011; 11:35.
  27. Foronjy RF, Mirochnitchenko O, Propokenko O, Lemaitre V, Jia Y, Inouye M, et al. Superoxide dismutase expression attenuates cigarette smoke- or elastase-generated emphysema in mice. *Amer J Respir Crit Care Med* 2006; 173(6):623–631.
  28. Ito S, Ingenito EP, Brewer KK, Black LD, Parameswaran H, Lutchen KR, et al. Mechanics, nonlinearity, and failure strength of lung tissue in a mouse model of emphysema: possible role of collagen remodeling. *J Appl Physiol* 2005; 98(2):503–511.
  29. Ishii M, Emami K, Xin Y, Barulic A, Kotzer CJ, Logan G a, et al. Regional Functional-Structure Relationships in Lungs of an Elastase Murine Model of Emphysema. *J Appl Physiol* 2012; 112:135–148.
  30. Sung JH, Yang H-M, Park JB, Choi G-S, Joh J-W, Kwon CH, et al. Isolation and characterization of mouse mesenchymal stem cells. *Transplant Proc* 2008; 40(8):2649–2654.
  31. Dominici M, Le Blanc K, Mueller I, Slaper-Cortenbach I, Marini F, Krause D, et al. Minimal criteria for defining multipotent mesenchymal stromal cells. The International Society for Cellular Therapy position statement. *Cytotherapy* 2006; 8(4):315–317.
  32. Lama V, Smith L, Badri L. Evidence for tissue-resident mesenchymal stem cells in human adult lung from studies of transplanted allografts. *J Clin Invest* 2007; 117(4):989–996.
  33. Tibboel J, Joza S, Reiss I, Jongste JC De, Post M. Amelioration of hyperoxia-induced lung injury using a sphingolipid-based intervention. *Euro Respir J* 2013; 42(3):e–pub ahead of print.
  34. Tsuchida S, Engelberts D, Roth M, McKerlie C, Post M, Kavanagh BP. Continuous positive airway pressure causes lung injury in a model of sepsis. *American journal of physiology. Lung Cell Mol Physiol* 2005; 289(4):L554–564.
  35. Ridsdale R, Roth-Kleiner M, D'Ovidio F, Unger S, Yi M, Keshavjee S, et al. Surfactant palmitoylmyristoylphosphatidylcholine is a marker for alveolar size during disease. *Amer J Respir Crit Care Med* 2005; 172(2):225–232.
  36. Emami K, Chia E, Kadlecsek S, Macduffie-Woodburn JP, Zhu J, Pickup S, et al. Regional correlation of emphysematous changes in lung function and structure: a comparison between pulmonary function testing and hyperpolarized MRI metrics. *J Appl Physiol* 2011; 110(1):225–235.
  37. Vanoirbeek J a J, Rinaldi M, De Vooght V, Haenen S, Bobic S, Gayan-Ramirez G, et al. Noninvasive and invasive pulmonary function in mouse models of obstructive and restrictive respiratory diseases. *American journal of respiratory cell and molecular biology*. 2010 Jan;42(1):96–104.
  38. Hamakawa H, Bartolák-Suki E, Parameswaran H, Majumdar A, Lutchen KR, Suki B. Structure-function Relations in an Elastase-induced Mouse Model of Emphysema. *Amer J Respir Cell Mol Biol* 2010; (C):1–38.
  39. Glaab T, Taube C, Braun A, Mitzner W. Invasive and noninvasive methods for studying pulmonary function in mice. *Respir Res* 2007; 8:63.
  40. Peták F, Habre W, Donati Y. Hyperoxia-induced changes in mouse lung mechanics: forced oscillations vs. barometric plethysmography. *J Appl Physiol* 2001; (90):2221–2230.
  41. De Vleeschauwer SI, Rinaldi M, De Vooght V, Vanoirbeek JA, Vanaudenaerde BM, Verbeken EK, et al. Repeated invasive lung function measurements in intubated mice: an approach for longitudinal lung research. *Lab Anim* 2011; 45(2):81–89.
  42. Zhen G, Xue Z, Zhao J, Gu N, Tang Z, Xu Y, et al. Mesenchymal stem cell transplantation increases expression of vascular endothelial growth factor in papain-induced emphysematous lungs and inhibits apoptosis of lung cells. *Cytother (Informa Healthcare Stockholm)* 2010; 12(5):605–614.
  43. Shigemura N, Okumura M, Mizuno S, Imanishi Y, Nakamura T, Sawa Y. Autologous transplantation of adipose tissue-derived stromal cells ameliorates pulmonary emphysema. *Amer J Transplant* 2006; 6(11):2592–2600.
  44. Bauer J, Liebisch G, Hofmann C, Huy C, Schmitz G, Obermeier F, et al. Lipid alterations in experimental murine colitis: role of ceramide and imipramine for matrix metalloproteinase-1 expression. *PLoS One* 2009; 4(9):e7197.
  45. Wright T, Notter R, Wang Z, Harmsen A, Gigliotti F. Pulmonary inflammation disrupts surfactant function during *Pneumocystis carinii* pneumonia. *Infect Immun* 2001; 69(2):758–764.
  46. Enhorning G, Hohlfeld J, Krug N, Lema G, Welliver RC. Surfactant function affected by airway inflammation and cooling: possible impact on exercise-induced asthma. *Euro Respir J: Euro Soc Clin Respir Physiol* 2000; 15(3):532–538.
  47. Liu M, Wang L, Enhorning G. Surfactant dysfunction develops when the immunized guinea-pig is challenged with ovalbumin aerosol. *Clin Exper Allergy: J Brit Soc Allergy Clin Immunol* 1995; 25(11):1053–1060.
  48. Peinado VI, Pizarro S, Barberà JA. Pulmonary vascular involvement in COPD. *Chest* 2008; 134(4):808–814.
  49. Matsuura Y, Kawata N, Yanagawa N, Sugiura T, Sakurai Y, Sato M, et al. Quantitative assessment of cross-sectional area of small pulmonary vessels in patients with COPD using inspiratory and expiratory MDCT. *Euro J Radiol* 2013; 82:1804–10.
  50. Barberà JA, Riverola A, Roca J, Ramirez J, Wagner PD, Ros D, et al. Pulmonary vascular abnormalities and ventilation-perfusion relationships in mild chronic obstructive pulmonary disease. *Amer J Respir Crit Care Med* 1994; 149(2 Pt 1):423–429.
  51. Peinado VI, Barberà JA, Abate P, Ramirez J, Roca J, Santos S, et al. Inflammatory Reaction in Pulmonary Muscular Arteries of Patients with Mild Chronic. *Am J Respir Crit Care Med* 1999; 159:1605–1611.
  52. Artaechevarria X, Blanco D, de Biurrun G, Ceresa M, Pérez-Martín D, Bastarrika G, et al. Evaluation of micro-CT for emphysema assessment in mice: comparison with non-radiological techniques. *Euro Radiol* 2011; 21(5):954–962.